

Article

The Properties and Durability of Self-Leveling and Thixotropic Mortars with Recycled Sand

Sebastiano Candamano ^{1,*}, Francesco Tassone ², Ivan Iacobini ¹, Fortunato Crea ¹ and Piero De Fazio ³

¹ Department of Mechanical, Energy and Management Engineering, University of Calabria, 87036 Rende, Italy; iacobini.ivan@gmail.com (I.I.); f.crea@unical.it (F.C.)

² Personal Factory S.p.A., 89822 Simbario, Italy; francesco.tassone@isolmix.com

³ Department of Energy Technology, DTE SAEN, Centro Ricerca ENEA Trisaia, 75026 Rotondella, Italy; piero.defazio@enea.it

* Correspondence: sebastiano.candamano@unical.it

Featured Application: In the present work, the authors investigated the properties and durability of mortars produced by replacing 100% of natural sand with recycled aggregate. The mix was tuned to produce self-leveling and thixotropic mortars that can find application in creating smooth and level surface/floor and in restoration.

Abstract: In recent decades, relevant environmental and economic reasons have driven an increasing interest in using a large amount of recycled aggregate in replacement of natural ones to produce mortar and concrete. The present study aims to investigate the effect of substituting 100% of natural sand with recycled aggregate on fresh properties, mechanical properties, and the durability of a thixotropic and a self-leveling mortar. Recycled aggregate was characterized using X-ray diffractometry and energy-dispersive X-ray spectroscopy. Its morphology was investigated using scanning electron microscopy and automated morphological imaging. Recycled aggregate mortars showed a moderate decline in initial workability, as well as higher shrinkage and porosity than the control ones. The compressive strength of self-leveling mortars produced with recycled aggregate was only 6% lower than mortars produced with natural sand. The gap increased to 40% in the case of thixotropic mortars. The self-leveling recycled aggregate mortar showed equivalent resistance to freeze–thaw cycles and better sulfate resistance than the control one. The thixotropic recycled aggregate mortar showed comparable sulphate resistance and only slightly lower resistance to freeze–thaw cycles than the control one. Their capacity to relief stresses, due to hydraulic pressures and the formation of expansive products, arises from their higher porosity. Thermal stability of the prepared mortars, after a curing period of 90 days, up to 700 °C, was also investigated. A significant decrease in ultrasonic pulse velocity is observed in the 200–400 °C interval for all the mortars, due to the dehydration–dehydroxylation of calcium silicate hydrate. The overall decline in the strength of both the recycled aggregate mortars was comparable to the control ones. The results reported in the present investigation suggest that the selection of high-quality recycled aggregate helps to obtain good-quality mortars when a large amount of natural sand is replaced.

Keywords: recycled aggregate mortar; mechanical properties; high temperature; sulphate resistance; freeze–thaw resistance



Citation: Candamano, S.; Tassone, F.; Iacobini, I.; Crea, F.; De Fazio, P. The Properties and Durability of Self-Leveling and Thixotropic Mortars with Recycled Sand. *Appl. Sci.* **2022**, *12*, 2732. <https://doi.org/10.3390/app12052732>

Academic Editor: Asterios Bakolas

Received: 24 January 2022

Accepted: 4 March 2022

Published: 7 March 2022

Publisher's Note: MDPI stays neutral with regard to jurisdictional claims in published maps and institutional affiliations.



Copyright: © 2022 by the authors. Licensee MDPI, Basel, Switzerland. This article is an open access article distributed under the terms and conditions of the Creative Commons Attribution (CC BY) license (<https://creativecommons.org/licenses/by/4.0/>).

1. Introduction

The construction industry consumes around 40% of all extracted natural resources, produces large amount of waste from building demolition, and consumes a lot of energy [1]. Several approaches have been carried out to mitigate the environmental impact of construction practices, such as investigating on more sustainable binders [2,3] and reusing demolition waste [4,5]. The generation of construction and demolition waste (C&DW) comprises the largest waste stream in the European Union (EU). It totaled 374 million

tons in the EU in 2016, excluding excavated soil [6]. Their management is driven by the increasingly environmental concerns about the over-exploitation of aggregates from quarries or rivers, landfill shortages, and rising transportation and landfill costs. Construction and demolition represent a priority area in the EU according to the Circular Economy Action Plan (EC 2015) for closing the loop, and EU countries set a 70% recovery target of C&DW within 2020 [6]. While most EU countries are on track to meet or exceeded the recovery target of 2020, it should be emphasized that most of the recovery practices result in a down-cycling [6]. They are actually based on low-value backfilling operations, such as filling holes on construction sites and low-grade recovery (involving the use of recycled and crushed cement or stones (aggregates) in road construction). The revised Waste Framework Directive (WFD 2008/98/EC, amended 2018/851) encourages measures which promote and implement selective demolition and sorting systems for C&DW in order to enable the removal and safe handling of hazardous substances and to facilitate reuse and high-quality recycling. Analyses of the costs and benefits of reusing demolition waste as recycled aggregates have been published in recent years, not only involving economic considerations but also environmental benefits. Tam [7] reported that the long-term net benefit of producing coarse recycled concrete aggregate (CRCA) from waste concrete was positive with a value of USD 22,334,116 per year, while that of crushed coarse natural aggregate (CNA) had a negative net value of USD −31,841,109 per year. Hameed [8] reported cost savings of 63.13% for recycled aggregate concrete (RAC) produced from the recycling of concrete waste to make fresh concrete at the same demolition site, rather than producing conventional concrete made with CNA. According to Ohemeng et al. [9], the long-term cost of producing one ton of coarse recycled concrete aggregate is about 40% less than that for coarse natural aggregate. Furthermore, they calculated that the environmental benefit of producing one ton of recycled concrete aggregate was approximately 97% higher than that for natural aggregate.

Marius Dan Gavrilitea [10] and Leal Filho [11] summarized the major environmental impacts and consequences of sand exploitation based on the analysis of existing literature associated with this issue. The very high volume of sand being currently extracted has a serious negative impact on rivers, deltas, and coastal and marine ecosystems, such as the loss of land through river or coastal erosion, the lowering of water levels, and the loss of sediment supply, thus damaging fauna and flora at significant levels.

However, technical and commercial barriers for circular concrete recycling can be summarized as follows:

- A lack of quality/purity in recycled materials;
- A lack of national instructions for recycling in new concrete in some countries;
- Low replacement rates in low-grade concrete allowed by Standards;
- A lack of documented information available regarding the origins of waste;
- Variable quality of feedstock;
- Contamination risks;
- A lack of trust of end-users in the quality/purity of recycled materials;
- The low price of virgin materials;
- The processing costs of demolition waste to secure high-quality material for recycling.

Different levers can be implemented to make the C&DW recycling an economically attractive option that includes levies on virgin materials, taxes on landfilling waste, and agreements and commitments between stakeholders in the value chain [6].

Specifically, to make the recycled aggregates competitive with virgin materials, it is crucial to increase their market value and manufacture products that perform as well as those made with virgin materials, or at least meet high-performance and durability criteria. The amount of recycled materials in cementitious composites and their applications is regulated by national standards. Furthermore, up to 20 percent substitution of virgin aggregates is allowed in new concrete because it does not damage the durability and the resistance of the cementitious materials. More than 50 percent substitution of virgin aggregates is only suitable for certain applications [12].

The possibility of using higher replacement rates of recycled aggregate from building demolition in concrete would represent a key step in increasing its high-quality recycling, due to the huge volumes of concrete yearly produced and being the fine and coarse aggregate accounting for 60–75% of concrete total volume [13–15]. Therefore, the scientific community has sought to close the gap in knowledge related to the topic. Attributing the loss of fresh and hardened state properties of RAC to the higher porosity of sorted RA has been met with unanimous consensus due to its inherent defects, such as the existing of additional interfacial transition zones (ITZ) [16–18]. These pores absorb water during mixing and have any load carrying capacity in the cured concrete. They also reduce the durability of RAC, because channels facilitate the penetration of detrimental substances, such as chloride ion and carbon dioxide, which both promote the corrosion of steel rebar and sulphate ion.

The mechanical properties and long-term performance of RAC can be improved by enhancing the properties of the ITZ to facilitate the reuse of RCA in construction projects. In the most recent papers, three group of approaches have been proposed and investigated:

- (1) Reduction in the recycled aggregate porosity:
 - Accelerated carbonation. The old mortar layer on the RAs contains a high amount of calcium hydroxide and calcium silicate hydrate. The method involves a carbonation reaction with CO_2 under the presence of water. The corresponding carbonated products show a volume expansion and partially occupy or even close the porosity of the RAs [19,20].
 - Biodeposition. The biodeposition is defined as microbial carbonate precipitation that can be achieved by ureolytic bacteria *B. Megaterium* [21] and *B. Sphaericus* [22]. The concrete pores can be filled with the insoluble calcium carbonate.
 - The addition of pozzolana. Silica fume (SF), fly ash (FA), and nano- SiO_2 (NAS) have been investigated for RA modification throughout the literature [23,24]. In this case, the pores are filled by the calcium silicate hydrate (C-S-H) gel produced by the pozzolana reaction with $\text{Ca}(\text{OH})_2$.
 - The addition of nanoparticles. Nanoparticles have much smaller size than cement grains. They not only act as filler in the ITZ, pores, or cracks, thus reducing the porosity, but also participate to the hydration process of the cement as nucleation centers for the crystallization [25,26].
 - Polymer emulsions. When polymer emulsion is applied to RA, the polymer molecules can fill up the pores and cracks in the RA, especially in the attached mortar and the ITZ and the aggregate surfaces can be sealed [27,28]
- (2) Reduction in the old mortar layer on recycled aggregate surface:
 - Acid treatment. Pre-soaking of recycled concrete aggregate in HCl , H_2SO_4 , HNO_3 , and (CH_3COOH) solution at room temperature for programmed time reduces or removes the old mortar layer, as the alkaline mortar can be dissolved in acid solutions [29,30].
 - Thermal treatment. The heating of the recycled concrete causes the dehydration of old cement stone, which leads to the separation of old mortar layer from the aggregate particles [31].
- (3) Property improvement without recycled aggregate modification:
 - The mixing approach. This involves an atypical mixing of concrete components [32]. In the two-stage mixing approach (TSMA), the mixing water is divided into two portions. In the sand enveloped mixing approach (SEMA), sand and 75% of water are mixed at first, and then the cement is added. After further mixing, the remaining water and coarse aggregate are added. The aim of the approach is to generate a thin cement slurry on the surface of recycled concrete aggregate during the first water addition that covers pores and cracks of the recycled concrete aggregates.

- The addition of fiber. The addition of short monofilament fibers in RAC is aimed to control the cracks opening and propagation by the “fibre bridge effect”, thus overcoming the brittle failure mode of the RAC and increasing its tensile and flexural strength [33]

The effect of the above-mentioned different approaches on the RAC properties has been investigated in terms of fresh properties (workability), physical and chemical properties (i.e., density, carbonation depth, and chloride ion penetration), mechanical properties (i.e., compressive, flexural, and splitting tensile strength as well as elastic modulus), and long-term performance (i.e., freezing-thawing resistance, alkali-silica reaction resistance, and creep and dry shrinkage). The bio-deposition significantly improves the elastic modulus and compressive strength of the final RAC. Specifically, the compressive strength increased by about 16% and 10% for RAC using recycled concrete aggregate and recycled mixed aggregate, respectively [34]. However, the bacterial culture medium may affect the concrete hydration process and long-term performance [21]. Shi et al. [23] studied the improvement in compressive strength of recycled concrete aggregate constituent RAC through adding pozzolanic materials SF, FA, and NAS (pozzolana to cement ratio is 0.13). Increases in the compressive strength of RAC modified with SF, FA, and NAS were 55.2%, 39.4%, and 17.6%, respectively, over 28 days, i.e., higher compared with that of RAC without any modification. A small amount of nanoparticles can significantly improve RCA properties, but they can also increase the cost of concrete production. Furthermore, the dispersion of the nanoparticles in the composition is a critical issue and the proposed lab methods have limitations given the massive production of concrete [25]. The increases in compressive strength after 28 days for HCl, HNO₃, and H₂SO₄ treatment were 34.6%, 25.3%, and 17.6% for a 100% RA replacement ratio, respectively. However, they are dangerous, expensive, and far from eco-friendly. Furthermore, they can deteriorate concrete and promote the corrosion of steel rebar. The mixing approach is considered a practical method [35] because it can be easily implemented, it has low costs, and it can lead to a significant strength enhancement (up to 20%) of the RAC compressive strength. Katkhuda et al. [36] applied chopped basalt fibers in RAC with a 20% replacement ratio with recycled concrete aggregate. Increasing the weight fibers content from 0% to 1.5% on cement increased the splitting tensile strength and flexural strength by 40% and 61%, respectively. However, the incorporation of fibers could reduce the workability of fresh RAC, especially when they have a high aspect ratio [36,37]. Larbi et al. [38] reported that heating the recycled concrete aggregate to maximum 800 °C for 2 h can remove most of the attached old mortar; however, this treatment has a high-energy consumption. Kou et al. [39], using recycled concrete aggregates soaked in 10% PVA solution for 24 h, reduced the water absorption of recycled aggregate concrete by approximately 70.0%.

Other than the above-mentioned technical and production process limitations, social aspects, such as a public awareness and acceptance of the products from recycled materials by public, prevent their actual massive use or commercialization [40]. The practical application of RAC is still limited and its use in structural application is even more so [16]. According to the authors, cementitious products based on recycled aggregate for non-structural application could achieve better acceptance by public in the status quo. Several papers have been recently published on this topic. Restuccia et al. [41] investigated the effect of washing and sieving the recycled aggregate on the properties of a mortar produced according to standard UNI EN 196-1. Da Silva Neto et al. [42] studied the influence of the mortar fine recycled aggregate ratio and the mixing sequence on the behavior of mortars using modified Brazilian standard NBR 7215 and two-stage mixing approach (TSMA), while Katz et al. [43] investigated the effects on the fresh and hardened properties of a rendering mortar at different replacement ratios. Roque et al. [44] presented a study of incorporation at 0%, 20%, 50%, and 100% (by volume) of demolition waste aggregate (CDW) in rendering mortars and evaluated their workability, mechanical strength, water absorption, shrinkage, open porosity, and durability. Mora-Ortiz et al. [45] evaluated the performance of masonry mortar manufactured by replacing natural sand with pre-wetted

recycled fine aggregate (RFA) and using a commercial plasticizer. In all the aforementioned works, the performance of the cement mortars with recycled aggregate was investigated only as a function of the percentage of replacement or of the mixing approach method used. In few cases, a plasticizer was used to adjust the workability. A higher percentage of recycled aggregate lead to lower workability and mechanical properties, partially compensated by adopting the different mixing methods. However, the performance, fresh and hardened properties, and durability of most of the commercial mortars and concrete are achieved or altered by adding chemical admixtures. The type and amount of the used chemicals depend on the specific application of concrete and mortars. Chemical admixtures also alter physical, chemical, and surface chemical properties of the mortars' components. Therefore, they reasonably affect the performance of recycled aggregate mortar. Based on the aforementioned information, authors evaluated the fresh and hardened properties and the durability of two commercial products, a self-leveling and a thixotropic mortar, whose mix design includes two specific chemical admixtures kits. They compared the results with those obtained when their mix design was modified by replacing the 100% the natural sand with recycled aggregate.

Self-leveling mortars (SLMs) are building materials with the property of leveling by gravity. They can be used over a subfloor before the installation of floors as underlayment to smoothen out any surface and correct the irregularities that the concrete could have [46]. Their high fluidity, good flatness, high compressive strength, and thin leveling layer also make them ideal for finished flooring in large supermarkets, shopping malls, parking lots, factory workshops, and warehouses. Cements, fine aggregates, mineral fillers, and chemical admixtures compose conventional SLMs [47]. Portland cement (PC) is commonly used as binder. However, SLMs that contain it struggle to meet the early strength requirements and show cracks and curls that commonly appear at the corners and perimeter. The low early strength and serious drying shrinkage of PC are responsible of the behavior [48]. In order to avoid the aforementioned issues, binary or ternary cementitious systems containing PC, calcium aluminate cement (CAC) or sulphoaluminate cement (SAC), and calcium sulfate (CS) are used [47]. The chemical admixtures (water reducer, retarder, early strength agent, and stabilizer) represent another significant factor that can influence their performance and properties by prolonging the setting time and increasing the fluidity of SLMs. An essential additive component of mortar as a floor material is the redispersible powder (RP). This is prepared by spray-drying or other process of polymer emulsion. A very small amount of RP can deeply affect the properties and performance of SLMs. When the powder mixes with water, the polymer emulsion can significantly improve the fluidity, the wear resistance and flexural strength, the bond strength, the impact resistance, and the flexibility of self-leveling mortar [49,50]. However, an excessive amount of RP can reduce the compressive strength of SLMs [50].

Thixotropic mortars are commonly used for non-structural and structural restoring and smoothing of concrete. Their elastic modulus, drying shrinkage, and chemical permeability and compatibility with the damaged concrete must be taken into account. Cement-based or polymer-modified repair materials can be used [51]. The former includes grout, mortar, or concrete (containing Portland cement, aluminous cement, or silicate cement). They are characterized by properties similar to those of the original concrete, thus assuring a high compatibility. However, they cannot overcome the drawbacks of the original concrete, such as permeability, which can lead to cracking carbonization, rebar corrosion, and drying shrinkage, which can affect bonding strength and, thus, the overall efficacy of repairs. The latter consists of mortars that contain polymers, such as redispersible polymer powder. This improves the bonding strength of repairing mortar to the substrate, fills in capillary pores, enhances the freeze–thaw resistance, improve resistance to water and chemicals, and reduces surface cracking [51]. They also provide a protective film on the surfaces of aggregates, and form a link with the hydration products of cement. Furthermore, the addition of cellulose ethers provides high viscosity, air incorporation, and water retention [52]. These factors also prevent an excessive loss of water into the substrate,

which could cause failures in the mechanism of adhesion and improve the sag resistance of the mortar. The viscosity of the cellulose ether solution is responsible of the thickening effect of cellulose ether on cement-based materials.

In the present investigation, a self-leveling mortar and a thixotropic mortar containing 100% of recycled aggregate and specific chemical admixtures kits were produced. Their fresh and hardened state properties, such as workability, porosity, compressive and flexural strengths, and drying shrinkage, were evaluated. Freeze–thaw, sulphate, and thermal resistance of the prepared mortars were also investigated in order to assess their durability. Self-leveling and thixotropic mortar have the same mix design but that containing natural sand was used as a control group.

2. Materials and Methods

2.1. Materials

Cement of type CEM II/A-LL 42.5 R was used to manufacture mortars. This was produced in accordance with standard UNI EN 197-1. The cement particle size distribution, based on volume distribution, is: D50 = 19.84 μm ; D90 = 36.11 μm ; D10 = 8.414 μm . Its main components, in terms of oxides were SiO₂ = 18.61 wt%; Fe₂O₃ = 2.87 wt%; Al₂O₃ = 4.38 wt%; CaO = 60.60 wt%; MgO = 3.16 wt%; K₂O = 0.79 wt%; Na₂O = 0.35; MnO = 0.17 wt%; SO₃ = 2.83 wt%; TiO₂ = 0.2 wt%.

A natural siliceous sand was used in the experimental campaign to produce the control mortars. The recycled aggregate came from the demolition of a building used as a warehouse. The demolition waste was then sorted by obtaining approximately 60 m³, mainly consisting of bricks, lime and cementitious mortars, and concrete. High-quality aggregates were then produced by dry grinding and sieving.

Scanning electron microscopy energy-dispersive X-ray analysis was used to investigate the morphology and elemental composition of the sands. Analyses were carried out with the help of a computer-controlled field emission Phenom ProX, equipped with an energy-dispersive X-ray (EDX) spectrometer (Deben, Suffolk, UK). Before SEM observation, the samples were sputtered with gold to stop their non-conductive surfaces from changing, and images were acquired at 20 kV. The counting time for the EDX analysis was 120 s.

Shape, surface texture, and mineralogical composition of sands can markedly affect the fresh and hardened state properties of the produced mortars and their durability [53–55]. In Figure 1, the SEM analysis of recycled aggregate (RS) and natural sand (NS) are reported.

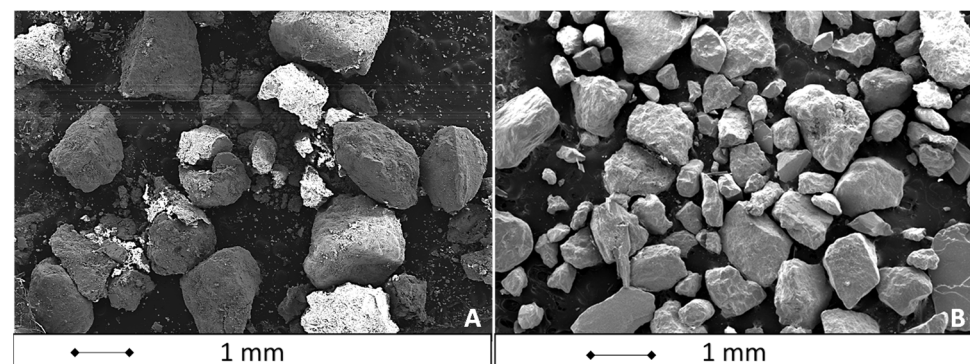


Figure 1. SEM analysis of recycled sand (A) and natural sand (B).

Natural sand (Figure 1B) is characterized by angular and rough grains. Recycled sand contains grains with irregular shape and sharply cut edges and some of grains show cracks throughout their microstructure (Figures 1A and 2). Their formation is promoted by the crushing process at the interfacial transition zone (ITZ) of concretes and mortars used as starting materials to produce RS, as reported by other authors [56,57].

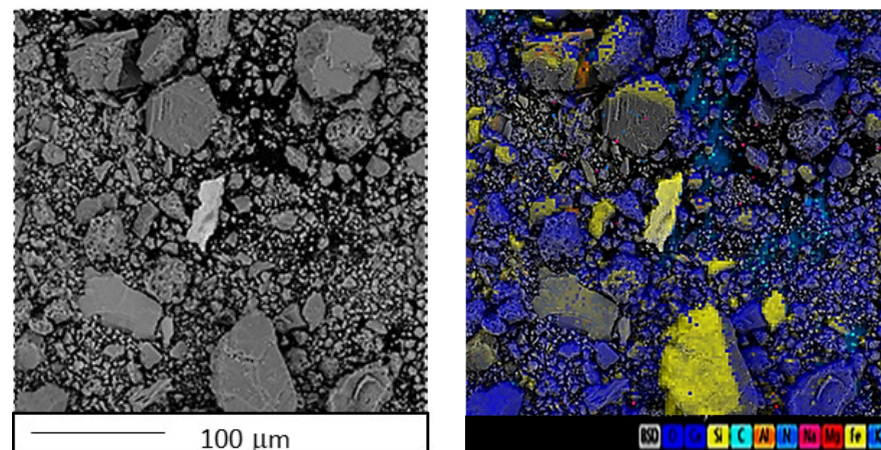


Figure 2. SEM-(left) and energy-dispersive X-ray mapping analysis (right) of recycled sand.

Natural sand is mainly composed by a silica, with other elements indicating the presence impurities (Table 1). The main elements found in the recycled aggregates (Table 1) are silicon, calcium, aluminium, and iron, originating from cementitious compounds (concretes and mortars) and bricks.

Table 1. The average composition of used sands in terms of oxides *.

Chemical Composition [%wt]	SiO ₂	Al ₂ O ₃	K ₂ O	Na ₂ O	CaO	FeO	MgO	SO ₃
Natural sand	57.8	11.7	1.9	2.7	17.5	5.2	3.1	0.2
Recycled sand	27.6	9.3	2.0	0.4	52.5	6.1	2.0	0.4

* Obtained by energy-dispersive X-ray analysis (EDX).

In Figure 2, the EDX mapping analysis of recycled sand is reported, revealing the heterogeneity of composition among grains.

Automated morphological imaging was carried out using Morphologi-G3 (MALVERN). This was used to investigate the recycled particles' shape; the circle equivalent (CE) diameter, defined as the diameter of a circle with the same area as the 2D image of the particle [58]; and the high sensitivity circularity (HS circularity) defined as:

$$\text{HS circularity} = 4\pi A/P^2$$

where A is the particle area and P is its perimeter [58]. HS circularity has values in the range 0–1. A perfect circle has a circularity of 1, while a 'spiky' or irregular object has a circularity value closer to 0. Representative results are reported in Figure 3.

The calculated HS circularity for RS, based on the analysis of more than 500,000 particles was 0.8. Recycled sand was analyzed by X-Ray diffractometry using a Rigaku MiniFlex 600 X-ray diffractometer (Rigaku Corporation, Tokyo, Japan) with CuK α (wavelength of 1.5406 Å) radiation generated at 20 mA and 40 KV. This was scanned at 0.02 2 θ step at a rate of 1°/min between 5° and 50° (2 θ angle range). The obtained X-Ray diffraction pattern is shown in Figure 4.

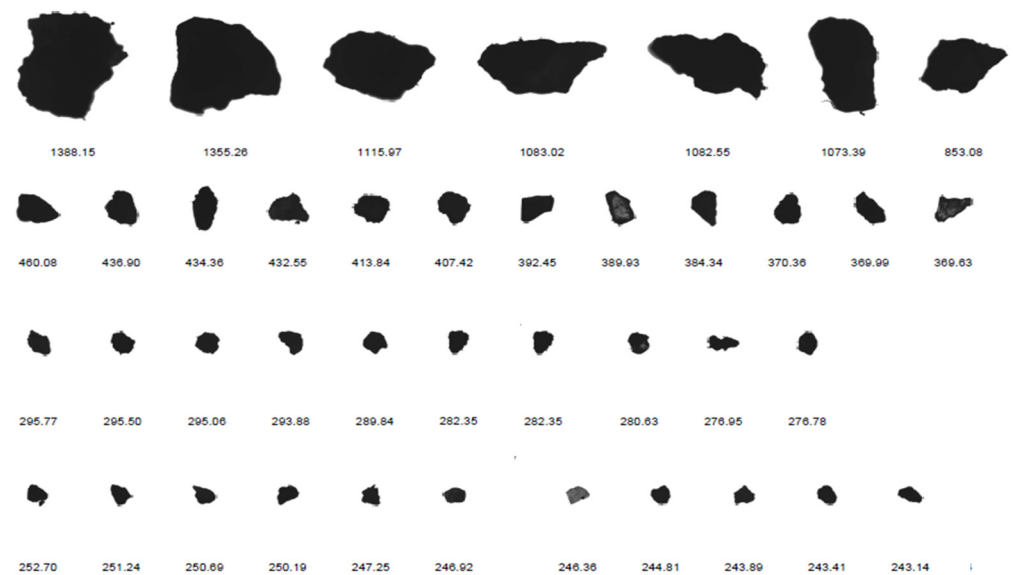


Figure 3. Particle images and CE diameters [μm] of RS as obtained by automated morphological imaging.

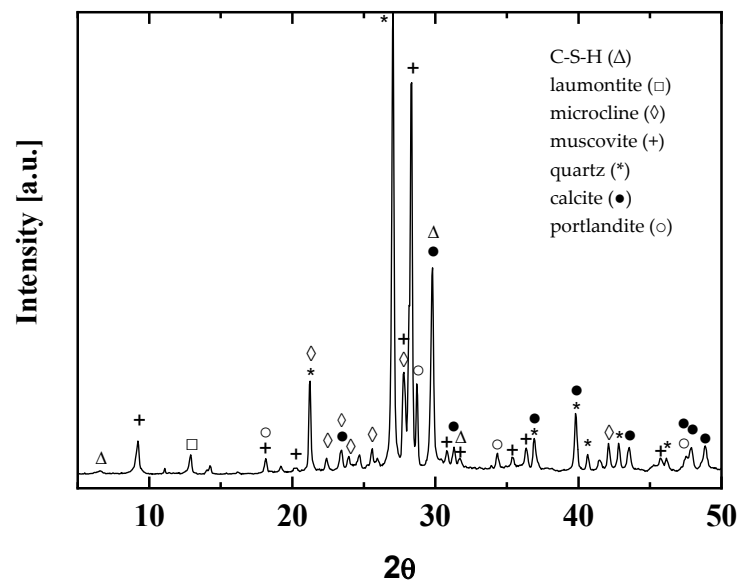


Figure 4. X-Ray diffraction pattern of recycled sand.

The main crystalline phases of the recycled sand are silicates, such as quartz (PDF 9000776), microcline (PDF 00-900-5308), calcite (PDF 7022027), portlandite (PDF 1000045), muscovite (PDF 00-900-6329), and laumontite (PDF R0601141). Significant peaks indicating the presence of calcium hydroxide and, its carbonated form, calcite are observed. The peaks of the quartz and feldspars are attributed to the natural sand and aggregates used in the manufacturing of the original concrete and mortar. Muscovite can be associated to the presence of bricks and ceramics. It is difficult to clearly distinguish the crystalline hydrated calcium silicate phases as their peaks overlap with the peaks of calcite and feldspars; however, the detection of calcium hydroxide is related to their occurrence. The results are in agreement with the chemical composition reported in Table 1; they are congruent with the mineralogical composition of the parent materials (concrete, mortar, and bricks) used for their production and they are consistent with other published studies [59–63].

Natural and recycled sands in a saturated surface dry (s.s.d.) condition were used to produce mortars. This prevents them from absorbing the free water that lends workability

to the mix [64,65]. The same particle size distribution curve, reported in Figure 5, was used for both the sands.

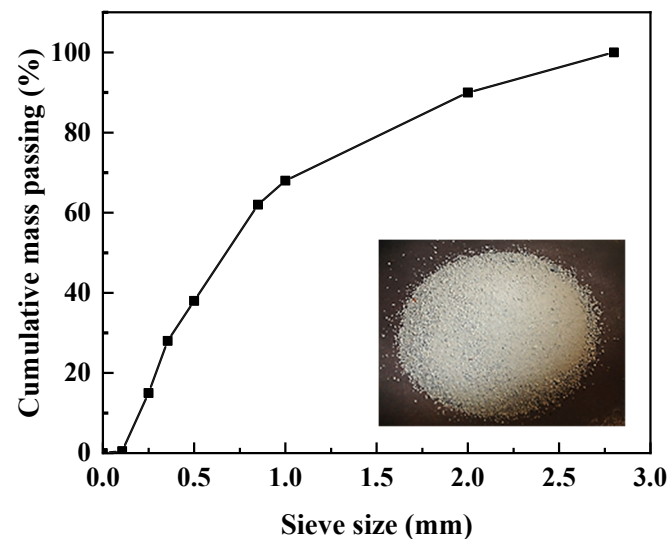


Figure 5. The grain size distribution curve of the natural and recycled aggregate.

By observing the granulometric curve of the aggregate, it can be highlighted that close attention was used to prevent fines used in the production of mortars. It is well known that fines from recycled aggregate have a considerable negative impact on mortars and concrete rheology. This is caused by their tendency to agglomerate when water is added to the mix, as different small forces (such as capillary and electrostatic charges, or van der Waals forces) arise [66–68]. Furthermore, they show some hydraulic activity and a rough surface that determine a high water absorption capacity [67].

2.2. Methods

Thixotropic and self-leveling mortars, with natural and recycled aggregates, were produced using a water/cement ratio equal to 0.52 and a sand/binder ratio equal to 2.28. Two chemical kits, especially those designed for producing self-leveling and thixotropic mortars, were provided by Personal Factory s.p.a. and used in the experimental campaign. The chemical kit was equal to the 5 wt% of the overall admixture. In Figure 6, the mix design of the four types of mortars is reported.

The mixing protocol establishes that water and cement are initially blended for 30 s. The chemical compound is then added and a further 30 s of blending is carried out. Natural or recycled sand is then added in 30 s under mixing, followed by 1 more minute of mixing time. The admixture rests for 1 min and 30 s and, finally, it is mixed again for 1 min before starting the tests.

For each type of mortar, the nomenclature used is classified as follows: the first two letters correspond to the origin of the aggregate, i.e., natural aggregate (NS) or recycled aggregate (RS); the last two letters refer to the type of mortar, i.e., thixotropic (RX) and self-leveling (PX).

At zero time after mixing, the workability of freshly prepared mortars was evaluated using the flow table and according to EN 1015-3 [69].

Several specimens, with a dimension of 40 mm × 40 mm × 160 mm, were produced according to EN 1015-11:2001 [70] and stored in a climatic chamber at 20 ± 3 °C and RH 90 ± 3% for certain cure ages. Compressive and flexural strengths, drying shrinkage, and open and total porosities were measured, according to relevant standard reported in Table 3. The drying shrinkage was measured on specimens stored in a dry environment (20 °C, RH 60%).

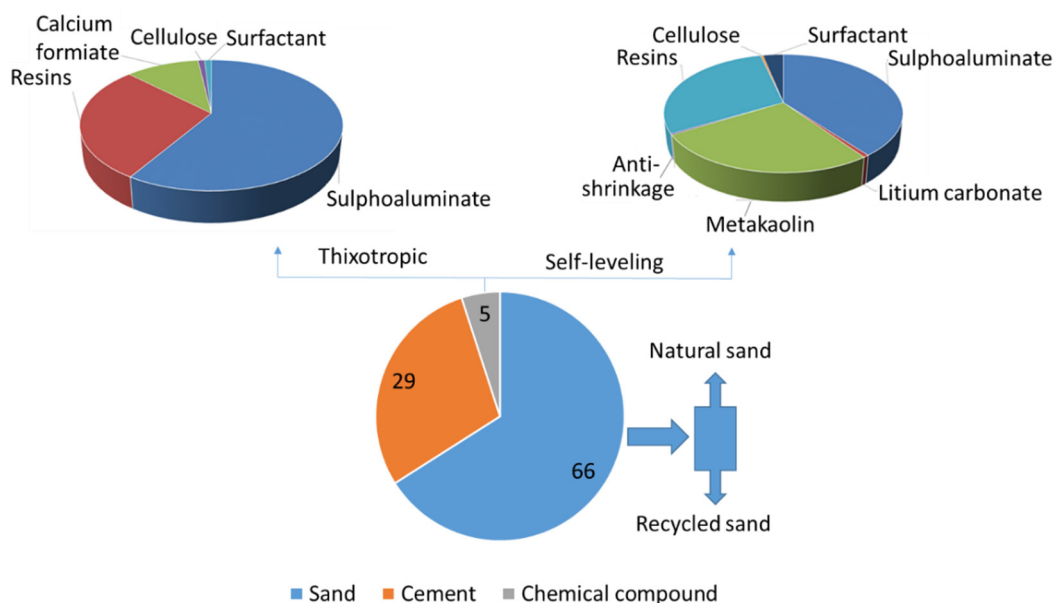


Figure 6. The mix design of thixotropic and self-leveling mortars.

Mixture proportions of mortars (kg/m³) are reported in Table 2.

Table 2. The mixture proportions of mortars (kg/m³).

	Cement [kg]	Natural Sand [kg]	Recycled Sand [kg]	Water [kg]	Chemical Kit [kg]
NSRX	539.3	1227.3	-	279.0	93
RSRX	496.0	-	1128.7	256.6	85.5
NRPX	539.3	1227.3	-	279.0	93
RSRX	496.0	-	1128.7	256.6	85.5

Table 3. Tests, shape and size of the specimens, curing time, and applied standards.

Test	Specimen Shape	Specimen Dimensions [cm]	Test Time [Days/Months/Cycles]	Standard
Workability	-	-	-	UNI EN 1015-3 [69]
Flexural strength	Prisms	4 × 4 × 16	2, 7, 28, 90 days	EN 1015-11 [70]
Compressive strength	Post bending test pieces	4 × 4 × 8	2, 7, 28, 90 days	EN 1015-11 [70]
Drying shrinkage	Prisms	4 × 4 × 16	2, 7, 28, 90 days	EN 12617-4 [71]
Open/total porosity	Prisms	4 × 4 × 16	28th curing day	UNI 11060:2003 [72]
Thermal cycles resistance	Prisms	4 × 4 × 16	-	-
Sulphate resistance	Prisms	4 × 4 × 16	6 months	UNI 8019 [73]
Freeze–thaw resistance	Prisms	4 × 4 × 16	300 cycles	UNI 7087 [74]

The resistance of the prepared mortars to freeze–thaw cycles was tested according to the relevant standard reported in Table 3, after a curing period of 28 days. Saturated specimens were placed in the freeze–thaw cycle test machine under the condition of freezing temperature of −20 °C and thawing temperature of 5 °C. Each cycle consisted of:

- (a) a cooling phase, in which the temperature moved from 5 °C (±2 °C) to −20 °C (±2 °C) at a constant rate of 5 °C/h (±0.5 °C/h);
- (b) a constant phase in which the temperature was kept constant at −20 °C (±2 °C) for two hours;
- (c) a heating phase in which the temperature returns to 5 °C (±2 °C) at the same velocity as step.

Mechanical properties and weight loss of specimens after 6 month of exposure to sulphate solutions were measured.

The resistance of the prepared mortars to sulphate was tested according to the relevant standard reported in Table 3, after a curing period of 28 days by soaking specimens in a solution containing 10% by weight of $MgSO_4$. The sulphate solution was replaced every 2 months.

The specimens' flexural and compressive strengths after 300 freeze–thaw cycles and their weight loss versus the number of freeze–thaw cycles, expressed as a percentage, were measured.

The thermal stability of the prepared mortars was also investigated by exposing the prismatic specimens, after a curing period of 90 days, at temperatures from 100 °C up to 700 °C in steps of 100 °C in a muffle furnace. Each thermal cycle consisted of a soaking period of 12 h followed by a cooling period of 24 h. The degradation of mechanical properties was evaluated by the non-destructive ultrasonic reflection technique. The mortars' compressive and flexural strengths, after all thermal cycles, were also measured and compared with those obtained with the untreated ones.

3. Results and Discussion

In Figure 7, the workability of the prepared mortars is reported.

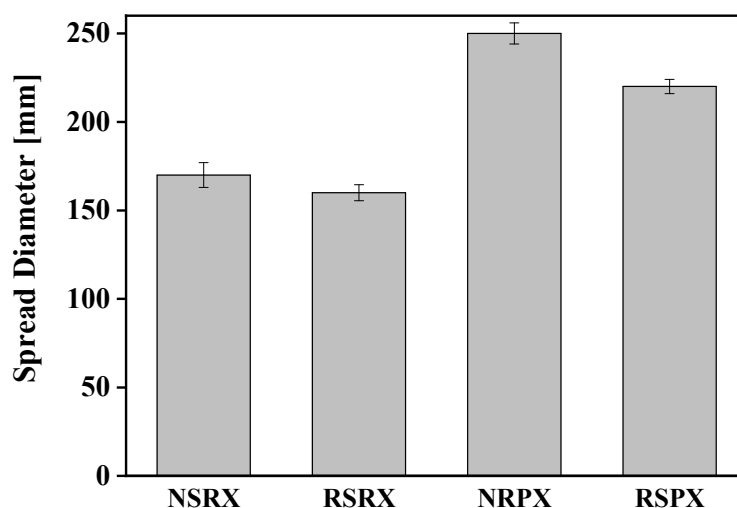


Figure 7. Spreading of thixotropic and self-leveling mortars produced with natural and recycled aggregate.

Both self-leveling and thixotropic mortars produced with RS show only a moderate decline in initial workability with respect to control mortars. It can be also observed that the decline in spreading value is lower in the case of the thixotropic mortar. As reported by many authors, several factors affect the workability of these types of mortars. A significant role is played by the RS content, the degree of saturation, the kinetics of water absorption, and the surface texture [53,54]. The chemical kit also has a pivotal role in defining their fresh state properties. When dry surface saturated aggregate is used, as in the present investigation, the more irregular and rougher surface of RS offers a higher resistance to the inter-particle movements, promotes particles' interlocking, and requires more water to be wetted [75]. The presence of adherent cement paste on aggregate, due to its porosity, also affects the workability [67]. The resin and surfactant included in the chemical kit of both the types of mortars limited the loss of workability by a ball bearing action and a dispersing effect, respectively. The higher amount of cellulose ethers (CE) in the chemical compound of the thixotropic mortars, used as viscosity enhancing and water retention additive to prevent the rapid loss of water by suction, hinders the wettability of the surface of recycled aggregate, thus lowering the gap in the initial mortar workability between NSRX and RSRX

mortars. The chemical kit used for self-leveling mortars, characterized by a higher amount of surfactant and a lower amount of cellulose, enhances the wettability of recycled sand surface, thus decreasing the initial workability in the RSPX mortar. In Figures 8 and 9, the evolution of compressive and flexural strengths of the prepared mortars with curing time is reported.

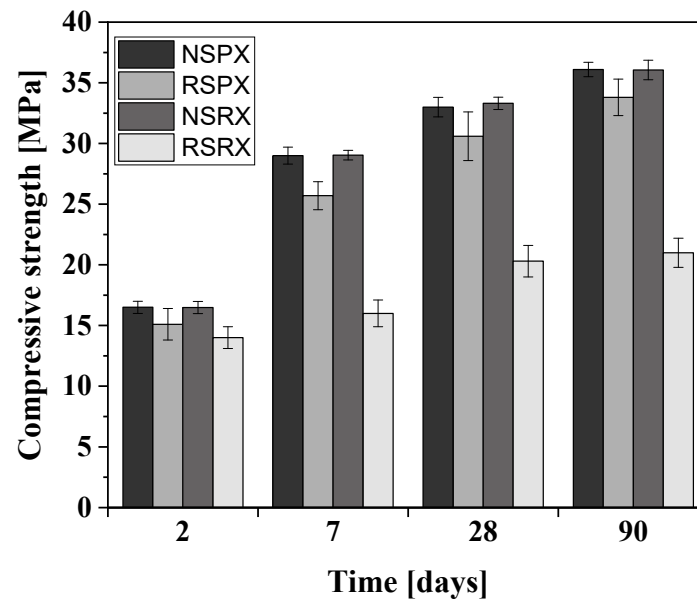


Figure 8. Compressive strength vs. curing days.

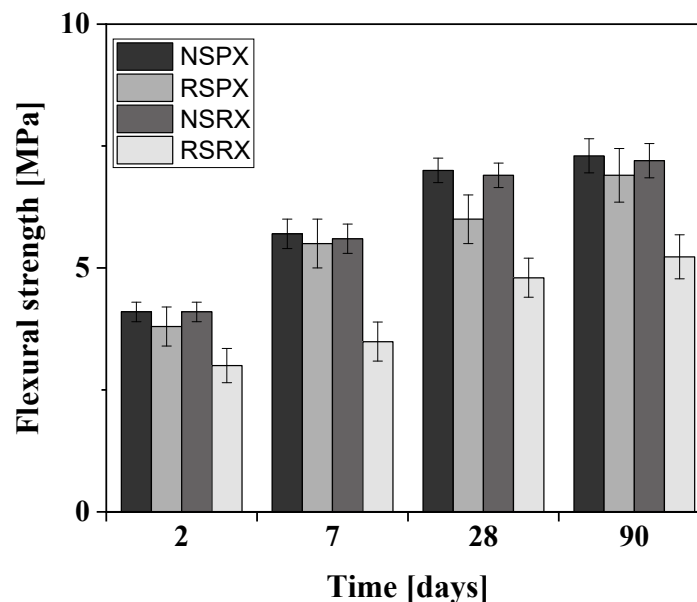


Figure 9. Flexural strength vs. curing days.

The compressive and flexural strengths of thixotropic (RSRX) and self-leveling (RSPX) mortars are lower than those of the corresponding control mortars made with siliceous sand. However, RSRX and RSPX show different behaviors, in terms of the extent of compressive strength decrease. The thixotropic RSRX mortar shows a compressive strength 15% lower than the reference mortar after two days of curing. The gap increases to around 40% after seven curing days and then remains stable for a longer curing time. The self-leveling RSPX mortar shows a limited compressive strength gap compared to the control mortar, varying from 11% to 6% with curing time. As reported by several investigations [76–80],

the reduction in mechanical properties in mortars produced using recycled aggregate can be caused by:

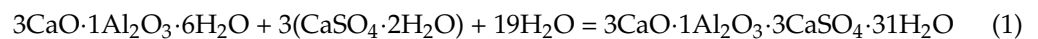
- the poorer mechanical properties of recycled sand in comparison to the natural sand used;
- the higher porosity of recycled sand;
- the presence of adherent cement paste on aggregate;
- the moisture conditions of aggregate;
- a weaker interfacial transition zone (ITZ).

As evidenced in Figures 1A and 2, the recycled sand, mainly composed by particles of mortar and concrete, shows micro-cracks occurring at the weaker interfacial transition zone (ITZ) because of the crushing process. They modestly participate, through the so-called “ceiling effect” [56], to lower the strength of the RSRX and RSPX mortars, in comparison to those with natural aggregates [81,82].

The chemical kit has an important role in explaining the different behavior of the two type of mortars with recycled sand.

It contains sulphoaluminate cement in the case of the thixotropic mortars, which has been partially replaced by metakaolin in the mix used to produce the self-leveling mortars.

Sulphoaluminate cement (CSA cement), used to provide a shorter setting time [83,84] and to lower the overall shrinkage, reacts according the following reaction:



The main hydration product of CSA cement is AFt (cf. Equation (1)). Its generation process requires a high amount of water.

Metakaolin reacts with the calcium hydroxide produced by the cement hydration reaction, which already exists in both the adherent cement paste on recycled aggregate and the recycled aggregate itself, as highlighted by X-Ray diffraction analysis (Figure 4). The pozzolanic reaction produces calcium silicate hydrate, thus increasing the density of the matrix especially the transition zone area between recycled aggregates and cement mortar and filling the porosity and the cracks of recycled aggregates, as revealed by Torkittikul and Chaipanich [85] and Zhao et al. [66].

The use of cellulose ethers (CE) and sulphoaluminate cement in the mix design of RSRX leads to an initial water retention, followed by faster consumption which produces expansive AFt. The addition of calcium formate reduces set times and improves early strengths by accelerating C-S-H formation. It is useful in repair systems, but further contributes to the fast water consumption. As an overall consequence, the wettability of adherent cement paste on recycled aggregate is partially hindered, the micro-cracks occurring in recycled aggregate can widen, the porosity increases, and mechanical performances decline.

In the chemical compound used for RSPX, the calcium formate is replaced by lithium carbonate, commonly used in the production of the self-leveling system, which only promotes fast setting. The partial replacement of sulphoaluminate cement with metakaolin leads to the reduced formation of expansive AFt and the densification of the transition zone in the recycled aggregates and between the cement paste and the recycled aggregate [85]. Therefore, the pore structure is improved, enhancing the mechanical performances, as reported in Figures 8 and 9.

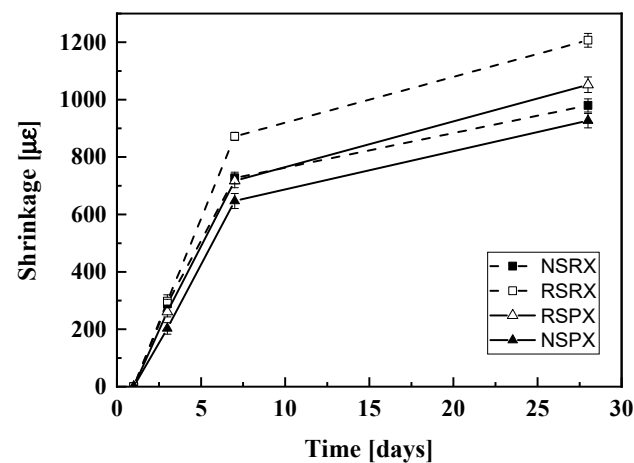
The porosity of the produced mortars was measured to validate the proposed explanation. Porosity is defined as the fraction of the total volume that is occupied by pores. It can be further classified into open porosity and closed porosity [86]. The difference between them is the interconnection of pores. The measure porosities are reported in Table 4.

Table 4. Open and total porosity of tested mortars.

Mixes	Open Porosity (%)	Total Porosity (%)
NSPX	17.3%	25.8%
RSPX	20.3%	32.6%
NSRX	20.5%	28.8%
RSRX	23.5%	35.56%

The higher porosity of the NSRX than NSPX can be attributed to the entrapped air due to the lower workability of the thixotropic mortar that can promote air entrapping. The RSRX and RSPX mortars show higher open and total porosities than NSRX and NRPX mortars, used as the control. Furthermore, the RSRX mortar has higher porosity than RSPX. The obtained results are consistent with the measured mortars' mechanical performances because, as expected, greater porosity is associated with lower strengths.

The drying shrinkage of the prepared mortars over early curing time is reported in Figure 10. All specimens experienced a continuous increase in shrinkage during the test period, with a fairly rapid growth during the first curing days, followed by a slower increase. Compared to the control mortars NSPX and NSRX, the RSPX and RSRX mortars show a shrinkage increase of 13.5% and 23.1%, respectively, after 28 days of curing. As expected, greater porosity leads total larger drying shrinkage. Similar results are reported in scientific literature by Mao et al. [87]. The frost resistance of mortars produced using recycled aggregate has been investigated in recent papers with divergent results that can be addressed to both the variability of the quality of the recycled aggregate and the different employed methods [88–92]. In order to further contribute to scientific literature, the prepared mortars were tested to freezing and thawing resistance. Mechanical properties were measured after 300 freeze–thaw (F-T) cycles, using the properties of mortars after 90 days of curing, corresponding with Figures 11 and 12.

**Figure 10.** The mortars' drying shrinkage vs. curing days.

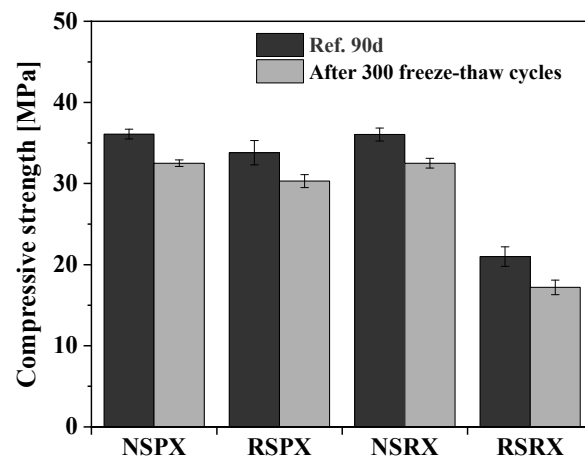


Figure 11. The mortars' compressive strength after 300 F-T cycles.

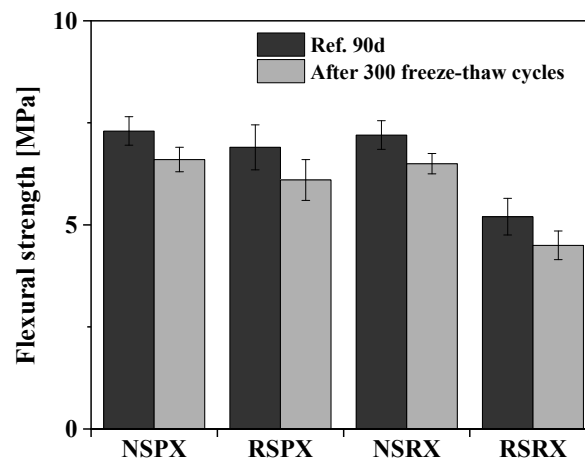


Figure 12. The mortars' flexural strength after 300 F-T cycles.

The final variation in the weight and mechanical performances is reported in Table 5.

Table 5. The weight and mechanical properties variation after freeze–thaw cycles and sulphate attack.

Mixes	Sulphate Attack (6 Months)				Freeze–Thaw Cycles (300 Cycles)		
	Δ Weight (%)	Δ Flexural Strength (%)	Δ Compressive Strength (%)	Penetration [cm]	Δ Weight (%)	Δ Flexural Strength (%)	Δ Compressive Strength (%)
NSPX	–16.9%	–63.0%	–80.6%	1.5	–1.0%	–9.6%	–10.0%
RSPX	–15.8%	–55.1%	–79.3%	1.7	–1.0%	–11.6%	–10.4%
NSRX	–12.5%	–69.4%	–86.1%	1.1	–1.7%	–9.7%	–9.8%
RSRX	–11.7%	–61.8%	–77.1%	1.2	–1.2%	–14.0%	–18.1%

The freezing and thawing resistance of RSPX is similar to that of the control mortar. The greater porosity that arises from the incorporation of the recycled aggregate favors the dissipation of hydraulic pressures. Only when the voids system is so developed that a significant decline in the initial mechanical properties can be determined, as for RSRX mortar, a slightly reduced resistance to F-T cycles is observed. The present investigation outcome confirms some previously reported findings [92–97].

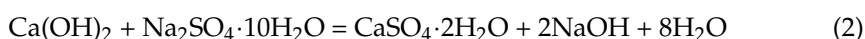
A sulphate attack is also a major concern for the durability of construction. Sulphate-rich environments expose mortar and concrete to expansion and degradation due to the formation of ettringite. It causes high internal stresses, leading to an extended cracking pattern [98,99].

The literature regarding recycled aggregate mortar and concrete performance against external sulphate attack (ESA) is not conclusive. This is mainly due to the several parameters involved in ESA. Kazmi et al. [30] replaced the coarse fraction of concrete with recycled aggregate and tested specimens after 60 days of immersion in sulfate solution. They reported a lower resistance of recycled aggregate concrete (RSC) compared to the control one in light of the sulphate attack, causing strength losses of around 26% and 20%, respectively. They attributed the findings to the higher porosity and water absorption of RSC, leading to higher sulphate ion penetration. However, some studies present a similar or even better performance for RSC than for natural aggregate mortar and concrete (NSC). Dhir et al. [100] reported that the exposure to a sulphate solution has a negative effect only for RSC with replacement ratios higher than 30%. Bulatovic et al. [101] reported that RSC with 100% replacement shows worse performance than NSC against ESA only when a high water-cement ratio ($w/c = 0.55$) and a non-sulphate-resistant cement were used.

Since the scientific community has reached no consensus by now, the prepared mortars have been tested for sulphate attack.

After an immersion period of 6 months, all the mortars experience a significant loss of mechanical properties (see Figures 13 and 14) that is explained by following reactions [102,103]:

- the formation of gypsum (calcium sulphate dihydrate), leading to softening and loss of concrete strength:



- The higher amount of gypsum converts tricalcium aluminate (C3A) in the mortars to ettringite (calcium aluminate trisulphate). The expansive reaction leads to high internal stresses and cracking:

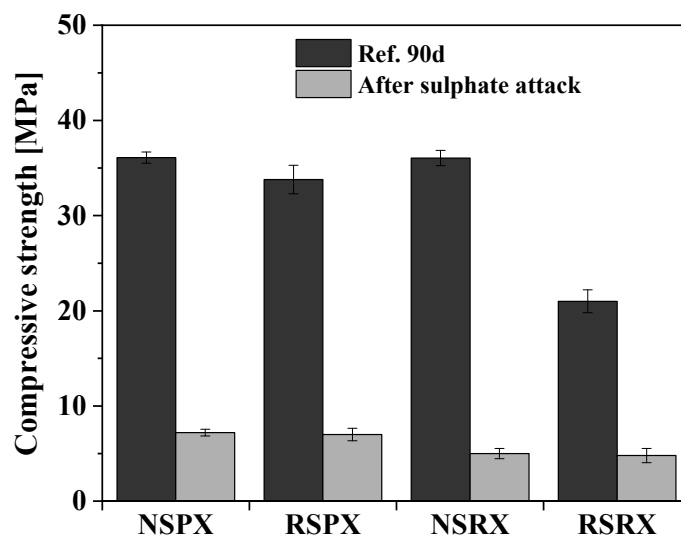


Figure 13. The mortars’ compressive strength after 6 months of immersion in sodium sulphate solution.

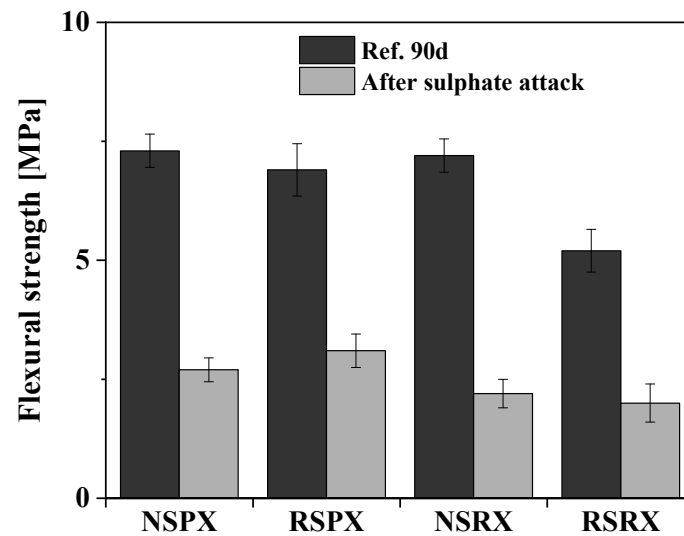


Figure 14. The mortars' flexural strength after 6 months of immersion in in sodium sulphate solution.

Notably, RSPX and NSPX showed a similar loss of compressive strength (Table 5), whereas RSRX mortar showed a better performance than the control mortar (NSRX).

The recycled aggregate used in the present campaign is mainly composed by cementitious compounds (concretes and mortars), as well as materials of ceramic origin (brick), as evidenced by EXD and X-Ray analyses. Therefore, mortars produced with the recycled aggregate contain more Portland cement hydration products which can react with external sulfate. Furthermore, as reported in Table 4, RSPX and RSRX mortars show increased overall porosities that favor and accelerate the ESA kinetics. The obtained results, thus, cannot be explained based on only these considerations and further contributions participate to define the observed behavior. According to authors, because ESA damage is mainly due to the formation of expansive products in confined pores, greater porosity can help to reduce the internal restriction of mortar to deform and decrease the generated internal stresses. The capacity of mortar and concrete produced with recycled aggregate to relief stresses due to their high porosity has been also reported by Santillán et al. [104] and Boudali et al. [105].

Figure 15 shows the cross-section of specimens exposed to sulphate attack post bending test and after using $\text{BaCl}_2 + \text{KMnO}_4$ solutions [106] to measure the sulphate penetration depth (Table 5).



Figure 15. Sulphate penetration depth in tested mortars, using $\text{BaCl}_2 + \text{KMnO}_4$ solutions and after 6 months of immersion in a sodium sulphate solution.

Recycled aggregate mortars show greater ion penetration depth than the control ones (Table 5). This can be explained by their higher open porosity. Interestingly, self-leveling mortars show higher sulphate ion penetration depths than the more porous thixotropic mortars. An important role in the observed behaviour can be attributed to a different efficiency in the redispersible powder dispersion. During mixing, polymer particles firstly disperse in the cement paste. As cement hydration proceeds and capillary water is consumed, the polymer particles flocculate to form a close-packed layer on the surfaces of capillary pores that can also effectively block the transportation of invasion ions based on the continuity polymer network [27]. The continuity polymer network depends on the amount and dispersion of the redispersible powder.

The exposure of cementitious materials to high temperatures, as it occurs during a fire, deteriorates their mechanical properties and affects their durability. The main causes of this decline can be ascribed to the decomposition of hydrates, the coarsening of porous structure, thermal cracking induced by water vapor pressure, and thermal mismatches [107,108]. The last two mechanisms considerably depend on the type of aggregate used in mortars [109]. Therefore, the thermal degradation characteristics of the prepared recycled aggregate mortars and the control ones were investigated by exposing the prismatic specimens, after a curing period of 90 days, up to 700 °C in steps of 100 °C in a muffle furnace. Each thermal cycle consisted of a soaking period of 12 h followed by a cooling period of 24 h. The degradation of the physical and mechanical properties was evaluated by the non-destructive ultrasonic reflection technique (Figure 16) and weight loss (Figure 17). Ultrasonic non-destructive testing (NDT-UT) techniques estimate the quality of mortar and concrete by measuring the propagation velocity of the ultrasonic wave [110]. Its magnitude depends on the material's density or the pore volume fraction; thus, it is closely related to their mechanical properties and modulus of elasticity [2].

The propagation velocities of the ultrasonic wave measured on specimens at room temperature and reported in Figure 16 are consistent with porosity and mechanical properties of the prepared mortars. In particular, a 5% difference between NSPX and RSPX and a 14% difference between NSRX and RSRX propagation pulse velocities (UPV) have been found. As the temperature increases (Figure 16), all the mortar experience a decrease in the propagation velocity as a consequence of the thermally induced damage. Four temperature intervals can be distinguished.

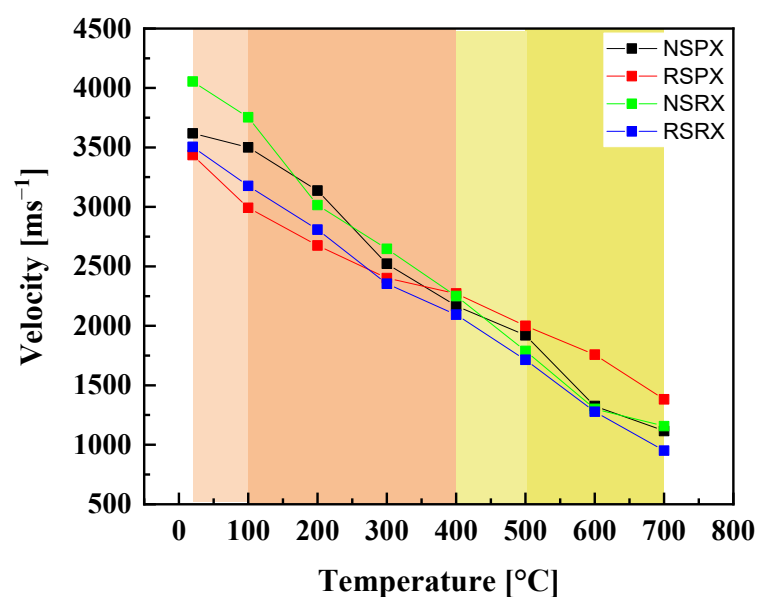


Figure 16. Propagation velocities of ultrasonic pulse vs. temperature for the tested mortars.

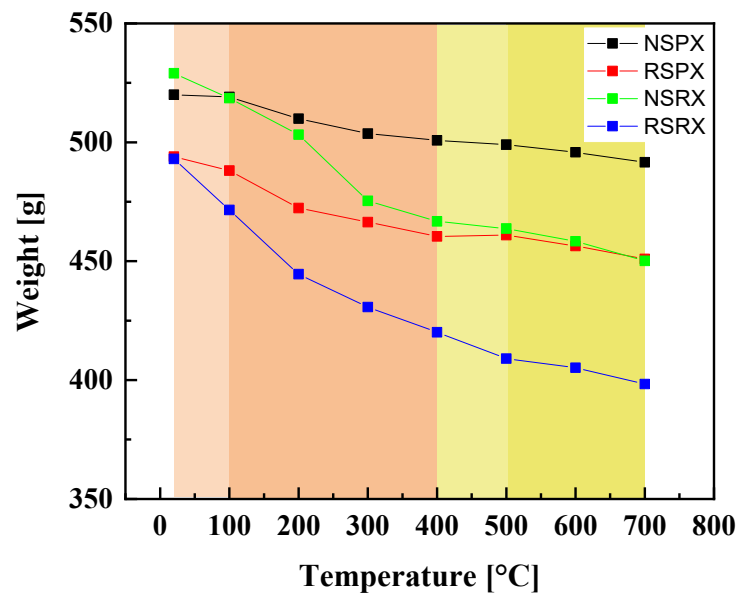


Figure 17. Weight of specimens vs. temperature for the tested mortars.

Interval 25–100 °C: the integrity of the specimen structure is close to that at room temperature. At these temperatures, the free water or capillary water inside the concrete are heated to evaporate and form water vapors. NSPX and NSRX mortars show a decrease in weight of 0.2% and 2%, respectively, which is lower than that of the corresponding mortars produced with recycled aggregate equal to 1.2% (RSPX) and 4.4% (RSRX) (Figure 17). This can be ascribed to the greater difficulty for water vapors to escape in more densely structured mortars [107]. The steeper decrease in UPV measured for RSPX (around 13%) and RSRX (9.3%) mortars can be explained by the greater ease of water vapor to escape in mortars that are more porous and of the fine-cracks to develop, under vapor pressure, from original defect of the recycled aggregate at pore boundaries.

Interval 100–400 °C: the capillary water continues to evaporate. Resins used as additive are thermally degraded. Furthermore, several reactions occur in the cement matrix. Ettringite (AFt) is thermally decomposed [110]; the dehydration–dehydroxylation of calcium silicate hydrate (C–S–H gel) cause the loss of crystal water and an increase in structural porosity. The loss of bonded water results in an increased weight loss for all the tested mortars, larger for mortars produced with recycled aggregate (5.6% for RSPX vs. 3.5% for NRPX and 10.4% for RSRX vs. 9.8% for NRSX). This finding can be explained by the following processes:

- The dehydration–dehydroxylation of calcium silicate hydrate (C–S–H gel) in RSPX and RSRX mortars not only involves the cement matrix, but also the recycled aggregate, mainly composed by concrete rubble.
- The higher amount of water vapor produced can easily escape in the more porous structures of mortars produced with recycled aggregate.

In this temperature range, a significant decrease in UPV is observed for all the mortars. However, it is steeper for mortars produced with natural sand (28.9% for RSPX vs. 36.9% for NRPX and 30.8% for RSRX vs. 37.1% for NRSX). This can be ascribed to their denser structure which hinders the migration of water vapors that are blocked and accumulated in the pores. The increased vapor pressure on pore boundaries favors the formation of fine cracks.

Interval 400–500 °C: the reactions of dehydration–dehydroxylation of calcium silicate hydrate (C–S–H gel) continue, and most of the calcium hydroxide (CH) decomposes into calcium oxide (CaO) [111,112]. The overall processes lead to an increase in weight loss and the formation of cracks in the mortar which determine a further lowering of measured UPV. No relevant deviations in the behavior of mortars are observed

Interval 500–700 °C: the reactions of dehydration–dehydroxylation of calcium silicate hydrate (C–S–H gel) involves the inner region of specimens. At about 570 °C, the α/β transition in the siliceous aggregates occurs with its related sudden volumetric expansion [113]. At about 650 °C, the thermal decomposition of calcium carbonate (CaCO_3) produced carbon dioxide (CO_2) starts [112]. The thermal expansion mismatch between the different minerals of the natural and recycled aggregate and cement matrix, the thermal expansion anisotropy within individual minerals, and the thermal decomposition of several components of the mortars and stress concentration due to water vapor reduce the compactness of all the mortars.

The residual mechanical properties of mortars after the thermal cycles are reported in Figures 18 and 19.

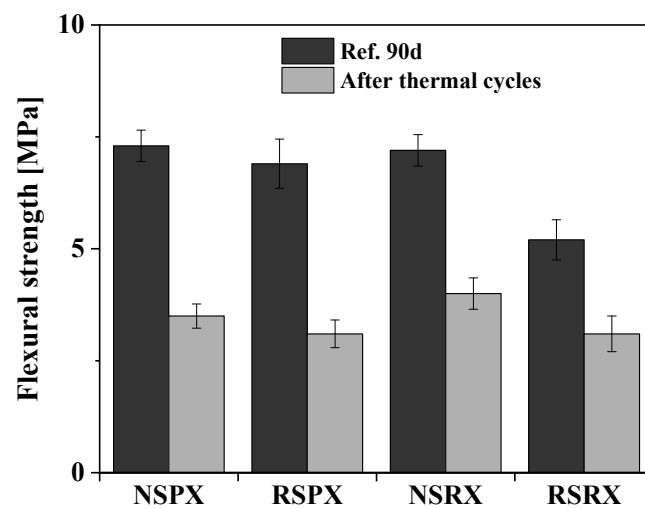


Figure 18. Flexural strength vs. temperature for the tested mortars.

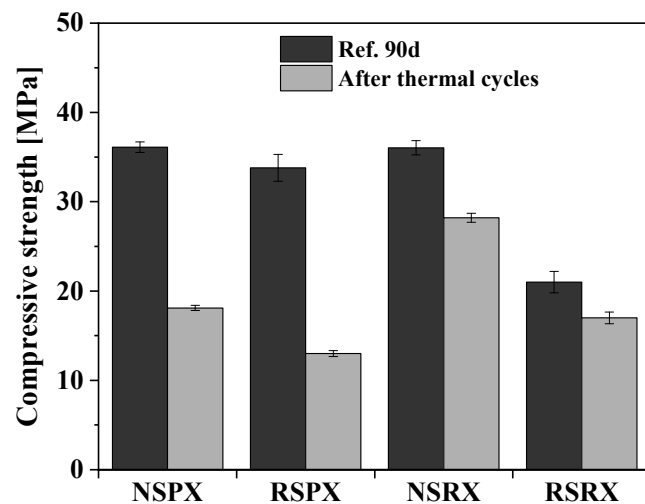


Figure 19. Compressive strength vs. temperature for the tested mortars.

Table 6 summarizes the variations in the weight and mechanical properties after thermal cycles.

The reduction in mechanical performances of the tested mortars containing 100% RS after exposure to thermal cycles up to 700 °C is comparable to that obtained for the control mortars, thus supporting the findings of Sarhat et al. [114] and Khaliq and Taimur [115].

Table 6. Variations in the weight and mechanical properties after thermal cycles.

Mixes	Δ Weight (%)	Δ Compressive Strength (%)	Δ Flexural Strength (%)
NSPX	−5.5%	−49.9%	−52.1%
RSPX	−8.7%	−61.5%	−55.6%
NSRX	−14.9%	−21.8%	−44.4%
RSRX	−19.2%	−19.0%	−40.7%

4. Conclusions

In this study, authors produced self-leveling and thixotropic mortars using 100%wt of recycled aggregate. Their physical and mechanical properties and their durability were investigated and compared with the control mortars. The following outcomes are stated below.

- The use of pre-saturated RS prevented the absorption of free water during the mixing. The workability of RSRX and RSPX mortars was 6% and 12% lower than that of the control mixes, respectively.
- The thixotropic and self-leveling mortars produced with recycled aggregate showed porosities of 35.6% and 32.6%, respectively. The higher porosity affected both their drying shrinkage behaviour and mechanical properties. In particular, RSRX mortars showed an increase of 23.1% in the drying shrinkage and a loss of about 40% in the compressive strength compared to the control mortar. RSPX mortar showed a loss of about 6% in the compressive strength and an increase of 13.5% in the drying shrinkage with respect to the control mix. The variation in properties was more pronounced in the thixotropic mortars, where the chemical additives contributed to the fast water consumption that partially hindered the wettability of adherent cement paste on recycled aggregate.
- After 300 freeze–thaw (F-T) cycles, RSRX and RSPX mortars, respectively, lost 11.6% and 14% of their initial compressive strength. Their greater porosity favours the dissipation of hydraulic pressures, resulting in a freezing and thawing resistance that is comparable to that of the control mortars, which experienced a loss of strength of about 10%.
- After a period of 6 months under sulphate attack, the self-leveling and thixotropic mortars with recycled aggregate showed a loss of compressive strength of about 55% and 62% respectively. Conversely, the decrease in the corresponding control mixes was 63% and 69%, respectively. The greater extent of porosity in RSRX and RSPX mortars, even favouring the ESA kinetics, reduces the internal restriction of mortar to deform and the generated internal stresses due to the formation of expansive products.
- The decline in the mortars' compressive strength containing recycled aggregate, after exposure at high temperatures up to 700 °C, is about 55% for RSPX and 19% for RSRX. This is comparable to that of the control mixes. In the 100–400 °C temperature range, a significant decrease in UPV, equal to 28.9% for RSPX, 36.9% for NRPX, 30.8% for RSRX, and 37.1% for NRSX, is observed and can be attributed to the dehydration–dehydroxylation of calcium silicate hydrate. Furthermore, a steeper decrease in UPV was measured in the 20–100 °C interval for mortars with recycled aggregate. This can be explained by the greater ease of water vapour to escape in mortars that are more porous and of the fine-cracks to develop, under vapour pressure, from the original defect of the recycled aggregate at the pore boundaries.

The present investigation shows that the use of high-quality and purity-recycled aggregates, obtained by selective demolition, can help to produce mortars with acceptable properties and durability, even when a high amount of natural sand is replaced.

Authors believe that a further tuning of the additives types and amount, the pre-treatment of the recycled aggregate to reduce the ceiling effect, and the partial replacement of Portland cement with pozzolanic powders could further improve the performance of the investigated mortars.

Author Contributions: Conceptualization, S.C., F.T. and F.C.; Data curation, S.C. and F.T.; Formal analysis, F.C. and P.D.F.; Investigation, S.C. and I.I.; Methodology, S.C., F.T. and I.I.; Validation, F.C. and P.D.F.; Writing—original draft, S.C.; All authors have read and agreed to the published version of the manuscript.

Funding: The ECOFIBAR project-PON 01_01522, funded by the Italian government, partially supported this work.

Conflicts of Interest: The authors declare no conflict of interest.

References

1. Bonoli, A.; Zanni, S.; Serrano-Bernardo, F. Sustainability in Building and Construction within the Framework of Circular Cities and European New Green Deal. The Contribution of Concrete Recycling. *Sustainability* **2021**, *13*, 2139. [[CrossRef](#)]
2. Coppola, L.; Coffetti, D.; Crotti, E.; Candamano, S.; Crea, F.; Gazzaniga, G.; Pastore, T. The combined use of admixtures for shrinkage reduction in one-part alkali activated slag-based mortars and pastes. *Constr. Build. Mater.* **2020**, *248*, 118682. [[CrossRef](#)]
3. Candamano, S.; Crea, F.; Iorfida, A. Mechanical characterization of basalt fabric-reinforced alkali-activated matrix composite: A preliminary investigation. *Appl. Sci.* **2020**, *10*, 2865. [[CrossRef](#)]
4. Martínez, P.S.; Cortina, M.G.; Martínez, F.F.; Sánchez, A.R. Comparative study of three types of fine recycled aggregates from construction and demolition waste (CDW), and their use in masonry mortar fabrication. *J. Clean. Prod.* **2016**, *118*, 162–169. [[CrossRef](#)]
5. Celikten, S.; Canbaz, M. Utilization of chrome ore concentration plant tailings as fine aggregate in ready mixed concrete. *J. Selcuk.-Tech.* **2018**, *2018*, 162–172.
6. Wahlström, M.; Bergmans, J.; Teittinen, T.; Bachér, J.; Smeets, A.; Paduart, A. *Eionet Report—ETC/WMGE 2020/1 Construction and Demolition Waste: Challenges and Opportunities in a Circular Economy*; European Environment Agency (EEA): Copenhagen, Denmark, 2020.
7. Tam, V.W. Economic comparison of concrete recycling: A case study approach. *Resour. Conserv. Recycl.* **2008**, *52*, 821–828. [[CrossRef](#)]
8. Hameed, M.; Chini, A. Impact of transportation on cost and energy for recycled concrete aggregate. In Proceedings of the ASC 46th Annual Meeting, Boston, MA, USA, 7–10 April 2010; pp. 187–194.
9. Ohemeng, E.A.; Ekolu, S.O. Comparative analysis on costs and benefits of producing natural and recycled concrete aggregates: A South African case study. *Case Stud. Constr. Mater.* **2020**, *13*, e00450. [[CrossRef](#)]
10. Gavrilitea, M.D. Environmental impacts of sand exploitation. Analysis of sand market. *Sustainability* **2017**, *9*, 1118. [[CrossRef](#)]
11. Leal Filho, W.; Hunt, J.; Lingos, A.; Platje, J.; Vieira, L.W.; Will, M.; Gavrilitea, M.D. The unsustainable use of sand: Reporting on a global problem. *Sustainability* **2021**, *13*, 3356. [[CrossRef](#)]
12. *European Standard EN, 206-1*; Specification, Performance, Production and Conformity. European Committee for Standardization: Brussels, Belgium, 2000.
13. Lotfi, S.; Rem, P.; Deja, J.; Mróz, R. An experimental study on the relation between input variables and output quality of a new concrete recycling process. *Constr. Build. Mater.* **2017**, *137*, 128–140. [[CrossRef](#)]
14. Xuan, D.; Zhan, B.; Poon, C.S. Assessment of mechanical properties of concrete incorporating carbonated recycled concrete aggregates. *Cem. Concr. Compos.* **2016**, *65*, 67–74. [[CrossRef](#)]
15. Wang, B.; Yan, L.; Fu, Q.; Kasal, B. A comprehensive review on recycled aggregate and recycled aggregate concrete. *Resour. Conserv. Recycl.* **2021**, *171*, 105565. [[CrossRef](#)]
16. Xie, T.; Gholampour, A.; Ozbakkaloglu, T. Toward the development of sustainable concretes with recycled concrete aggregates: Comprehensive review of studies on mechanical properties. *J. Mater. Civ. Eng.* **2018**, *30*, 04018211. [[CrossRef](#)]
17. Silva, R.V.; Brito, J.; de Dhir, R.K. Fresh-State performance of recycled aggregate concrete: A review. *Constr. Build. Mater.* **2018**, *178*, 19–31. [[CrossRef](#)]
18. Del Bosque, I.S.; Zhu, W.; Howind, T.; Matías, A.; De Rojas, M.S.; Medina, C. Properties of interfacial transition zones (ITZs) in concrete containing recycled mixed aggregate. *Cem. Concr. Compos.* **2017**, *81*, 25–34. [[CrossRef](#)]
19. Tam, V.W.; Butera, A.; Le, K.N.; Li, W. Utilising CO₂ technologies for recycled aggregate concrete: A critical review. *Constr. Build. Mater.* **2020**, *250*, 118903. [[CrossRef](#)]
20. Liang, C.; Pan, B.; Ma, Z.; He, Z.; Duan, Z. Utilization of CO₂ curing to enhance the properties of recycled aggregate and prepared concrete: A review. *Cem. Concr. Compos.* **2020**, *105*, 103446. [[CrossRef](#)]
21. Singh, L.P.; Bisht, V.; Aswathy, M.S.; Chaurasia, L.; Gupta, S. Studies on performance enhancement of recycled aggregate by incorporating bio and nano materials. *Constr. Build. Mater.* **2018**, *181*, 217–226. [[CrossRef](#)]
22. García-González, J.; Rodríguez-Robles, D.; Wang, J.; De Belie, N.; Morán-del Pozo, J.M.; Guerra-Romero, M.I.; Juan-Valdés, A. Quality improvement of mixed and ceramic recycled aggregates by biodeposition of calcium carbonate. *Constr. Build. Mater.* **2017**, *154*, 1015–1023. [[CrossRef](#)]
23. Shi, C.; Wu, Z.; Cao, Z.; Ling, T.C.; Zheng, J. Performance of mortar prepared with recycled concrete aggregate enhanced by CO₂ and pozzolan slurry. *Cem. Concr. Compos.* **2018**, *86*, 130–138. [[CrossRef](#)]

24. Luo, Z.; Li, W.; Tam, V.W.; Xiao, J.; Shah, S.P. Current progress on nanotechnology application in recycled aggregate concrete. *J. Sustain. Cem.-Based Mater.* **2019**, *8*, 79–96. [[CrossRef](#)]
25. Gao, C.; Huang, L.; Yan, L.; Jin, R.; Chen, H. Mechanical properties of recycled aggregate concrete modified by nano-particles. *Constr. Build. Mater.* **2020**, *241*, 118030. [[CrossRef](#)]
26. Lei, B.; Li, W.; Tang, Z.; Li, Z.; Tam, V.W. Effects of environmental actions, recycled aggregate quality and modification treatments on durability performance of recycled concrete. *J. Mater. Res. Technol.* **2020**, *9*, 13375–13389. [[CrossRef](#)]
27. Candamano, S.; Crea, F.; Coppola, L.; De Luca, P.; Coffetti, D. Influence of acrylic latex and pre-treated hemp fibers on cement based mortar properties. *Constr. Build. Mater.* **2021**, *273*, 121720. [[CrossRef](#)]
28. Shi, C.; Li, Y.; Zhang, J.; Li, W.; Chong, L.; Xie, Z. Performance enhancement of recycled concrete aggregate—A review. *J. Clean. Prod.* **2016**, *112*, 466–472. [[CrossRef](#)]
29. Saravanakumar, P.; Abhiram, K.; Manoj, B. Properties of treated recycled aggregates and its influence on concrete strength characteristics. *Constr. Build. Mater.* **2016**, *111*, 611–617. [[CrossRef](#)]
30. Kazmi, S.M.S.; Munir, M.J.; Wu, Y.F.; Patnaikuni, I.; Zhou, Y.; Xing, F. Effect of different aggregate treatment techniques on the freeze-thaw and sulfate resistance of recycled aggregate concrete. *Cold Reg. Sci. Technol.* **2020**, *178*, 103126. [[CrossRef](#)]
31. Akbarnezhad, A.; Ong, K.C.G.; Zhang, M.H.; Tam, C.T.; Foo, T.W.J. Microwave-Assisted beneficiation of recycled concrete aggregates. *Constr. Build. Mater.* **2011**, *25*, 3469–3479. [[CrossRef](#)]
32. Verian, K.P.; Ashraf, W.; Cao, Y. Properties of recycled concrete aggregate and their influence in new concrete production. *Resour. Conserv. Recycl.* **2018**, *133*, 30–49. [[CrossRef](#)]
33. Lei, B.; Li, W.; Liu, H.; Tang, Z.; Tam, V.W. Synergistic effects of polypropylene and glass fiber on mechanical properties and durability of recycled aggregate concrete. *Int. J. Concr. Struct. Mater.* **2020**, *14*, 37. [[CrossRef](#)]
34. Wang, C.; Xiao, J.; Zhang, G.; Li, L. Interfacial properties of modeled recycled aggregate concrete modified by carbonation. *Constr. Build. Mater.* **2016**, *105*, 307–320. [[CrossRef](#)]
35. Bai, G.; Zhu, C.; Liu, C.; Liu, B. An evaluation of the recycled aggregate characteristics and the recycled aggregate concrete mechanical properties. *Constr. Build. Mater.* **2020**, *240*, 117978. [[CrossRef](#)]
36. Katkhuda, H.; Shatarat, N. Improving the mechanical properties of recycled concrete aggregate using chopped basalt fibers and acid treatment. *Constr. Build. Mater.* **2017**, *140*, 328–335. [[CrossRef](#)]
37. Dong, J.F.; Wang, Q.Y.; Guan, Z.W. Material properties of basalt fibre reinforced concrete made with recycled earthquake waste. *Constr. Build. Mater.* **2017**, *130*, 241–251. [[CrossRef](#)]
38. Larbi, J.A.; Heijnen, W.M.M.; Brouwer, J.P.; Mulder, E. Preliminary laboratory investigation of thermally treated recycled concrete aggregate for general use in concrete. In *Waste Management Series*; Elsevier: Amsterdam, The Netherlands, 2000; Volume 1, pp. 129–139.
39. Kou, S.C.; Zhan, B.J.; Poon, C.S. Use of a CO₂ curing step to improve the properties of concrete prepared with recycled aggregates. *Cem. Concr. Compos.* **2014**, *45*, 22–28. [[CrossRef](#)]
40. Chi, B.; Lu, W.; Ye, M.; Bao, Z.; Zhang, X. Construction waste minimization in green building: A comparative analysis of LEED-NC 2009 certified projects in the US and China. *J. Clean. Prod.* **2020**, *256*, 120749. [[CrossRef](#)]
41. Restuccia, L.; Spoto, C.; Ferro, G.A.; Tulliani, J.M. Recycled mortars with C & D waste. *Procedia Struct. Integr.* **2016**, *2*, 2896–2904.
42. Silva Neto, G.A.D.; Leite, M.B. Study of the influence of the mortar fine recycled aggregate ratio and the mixing sequence on the behavior of new mortars. *Ambiente Construído* **2018**, *18*, 53–69. [[CrossRef](#)]
43. Katz, A.; Kulisch, D. Performance of mortars containing recycled fine aggregate from construction and demolition waste. *Mater. Struct.* **2017**, *50*, 199. [[CrossRef](#)]
44. Roque, S.; Maia Pederneiras, C.; Brazão Farinha, C.; de Brito, J.; Veiga, R. Concrete-Based and mixed waste aggregates in rendering mortars. *Materials* **2020**, *13*, 1976. [[CrossRef](#)]
45. Mora-Ortiz, R.S.; Munguía-Balvanera, E.; Díaz, S.A.; Magaña-Hernández, F.; Angel-Meraz, D.; Bolaina-Juárez, Á. Mechanical behavior of masonry mortars made with recycled mortar aggregate. *Materials* **2020**, *13*, 2373. [[CrossRef](#)] [[PubMed](#)]
46. Anderberg, A.; Wadsö, L. Drying and hydration of cement based self-leveling flooring compounds. *Dry. Technol.* **2007**, *25*, 1995–2003. [[CrossRef](#)]
47. Dong, W.; Fang, C.; Hu, R. Influence of Redispersible Powder on Properties of Self-Leveling Mortar of Ternary Cementitious System. *Materials* **2020**, *13*, 5703. [[CrossRef](#)] [[PubMed](#)]
48. Georgin, J.F.; Ambroise, J.; Péra, J.; Reynouard, J.M. Development of self-leveling screed based on calcium sulfoaluminate cement: Modelling of curling due to drying. *Cem. Concr. Compos.* **2008**, *30*, 769–778. [[CrossRef](#)]
49. Cui, J. *The Influence of Redispersible Powder on Mechanical Properties of EPS Light-Aggregate Concrete*. Applied Mechanics and Materials; Trans Tech Publications Ltd.: Stafa-Zurich, Switzerland, 2014; Volume 651, pp. 173–176.
50. Sun, S.B.; Li, J.J.; Zhao, L. The Effect of Re-Dispersible Polymer Powders on Cement-Based Self-Leveling Mortar. In *Key Engineering Materials*; Trans Tech Publications Ltd.: Stafa-Zurich, Switzerland, 2017; Volume 730, pp. 395–400.
51. Jung, K.C.; Chang, S.H. Evaluation of shrinkage-induced stress in a runway repaired using compliant polymer concrete. *Compos. Struct.* **2016**, *158*, 217–226. [[CrossRef](#)]
52. Sobala, M.; Nosal, K.; Pichniarczyk, P. Effect of methyl cellulose on the properties of adhesive cement mortars. *Cem. Lime Concr.* **2010**, *6*, 359–365.

53. Cortes, D.D.; Kim, H.K.; Palomino, A.M.; Santamarina, J.C. Rheological and mechanical properties of mortars prepared with natural and manufactured sands. *Cem. Concr. Res.* **2008**, *38*, 1142–1147. [[CrossRef](#)]
54. Maza, M.; Naceri, A.; Zitouni, S. Physico-Mechanical properties of mortar made with binary natural fine aggregates (dune sand and crushed sand) with and without chemical admixture. *Asian J. Civ. Eng.* **2016**, *17*, 663–682.
55. Lee, G.C.; Choi, H.B. Study on interfacial transition zone properties of recycled aggregate by micro-hardness test. *Constr. Build. Mater.* **2013**, *40*, 455–460. [[CrossRef](#)]
56. Le, T.; Le Saout, G.; Garcia-Diaz, E.; Betrancourt, D.; Rémond, S. Hardened behavior of mortar based on recycled aggregate: Influence of saturation state at macro-and microscopic scales. *Constr. Build. Mater.* **2017**, *141*, 479–490. [[CrossRef](#)]
57. Contreras, M.; Teixeira, S.R.; Lucas, M.C.; Lima, L.C.N.; Cardoso, D.S.L.; Da Silva, G.A.C.; Gregório, G.C.; de Souza, A.E.; Dos Santos, A. Recycling of construction and demolition waste for producing new construction material (Brazil case-study). *Constr. Build. Mater.* **2016**, *123*, 594–600. [[CrossRef](#)]
58. Hejduk, A.; Czajka, S.; Lulek, J. Impact of co-processed excipient particles solidity and circularity on critical quality attributes of orodispersible minitables. *Powder Technol.* **2021**, *387*, 494–508. [[CrossRef](#)]
59. Reis, G.S.D.; Quattrone, M.; Ambrós, W.M.; Grigore Cazacliu, B.; Hoffmann Sampaio, C. Current applications of recycled aggregates from construction and demolition: A review. *Materials* **2021**, *14*, 1700. [[CrossRef](#)]
60. Evangelista, L.; Guedes, M.; De Brito, J.; Ferro, A.C.; Pereira, M.F. Physical, chemical and mineralogical properties of fine recycled aggregates made from concrete waste. *Constr. Build. Mater.* **2015**, *86*, 178–188. [[CrossRef](#)]
61. Rodrigues, F.; Carvalho, M.T.; Evangelista, L.; De Brito, J. Physical–Chemical and mineralogical characterization of fine aggregates from construction and demolition waste recycling plants. *J. Clean. Prod.* **2013**, *52*, 438–445. [[CrossRef](#)]
62. Awoyera, P.O.; Okoro, U.C. Filler-ability of highly active metakaolin for improving morphology and strength characteristics of recycled aggregate concrete. *Silicon* **2019**, *11*, 1971–1978. [[CrossRef](#)]
63. Pederneiras, C.M.; Durante, M.D.P.; Amorim, Ê.F.; Ferreira, R.L.D.S. Incorporation of recycled aggregates from construction and demolition waste in paver blocks. *Rev. IBRACON Estrut. Mater.* **2020**, *13*, e13405. [[CrossRef](#)]
64. Hansen, T.C. (Ed.) *Recycling of Demolished Concrete and Masonry*; CRC Press: Boca Raton, FL, USA, 1992.
65. Tam, V.W.; Gao, X.F.; Tam, C.M. Microstructural analysis of recycled aggregate concrete produced from two-stage mixing approach. *Cem. Concr. Res.* **2005**, *35*, 1195–1203. [[CrossRef](#)]
66. Zhao, Z.; Remond, S.; Damidot, D.; Xu, W. Influence of fine recycled concrete aggregates on the properties of mortars. *Constr. Build. Mater.* **2015**, *81*, 179–186. [[CrossRef](#)]
67. González-Fontebo, B.; González-Taboada, I.; Carro-López, D.; Martínez-Abella, F. Influence of the mixing procedure on the fresh state behaviour of recycled mortars. *Constr. Build. Mater.* **2021**, *299*, 124266. [[CrossRef](#)]
68. Miranda, L.F.; Selmo, S.M. CDW recycled aggregate renderings: Part I—Analysis of the effect of materials finer than 75 µm on mortar properties. *Constr. Build. Mater.* **2006**, *20*, 615–624. [[CrossRef](#)]
69. *UNI EN 1015-3:2007*; Consistency of Wet Mortar. European Committee for Standardization: Brussels, Belgium, 2007.
70. *UNI EN 1015-11:2001*; Methods of Test for Mortar for Masonry—Determination of Flexural and Compressive Strength of Hardened Mortar. European Committee for Standardization: Brussels, Belgium, 1999.
71. *UNI EN 12617-4:2003*; Hydraulic Shrinkage of Cement Mortar Products and Systems for the Protection and Repair of Concrete Structures—Test Methods—Determination of Shrinkage and Expansion. European Committee for Standardization: Brussels, Belgium, 2003.
72. *UNI 11060:2003*; Cultural Heritage—Natural and Artificial Stones—Determination of Density and Voids. European Committee for Standardization: Brussels, Belgium, 2003.
73. *UNI 8019-4.3*; Determination of Sulfate Ions Penetration. European Committee for Standardization: Brussels, Belgium, 1979.
74. *UNI 7087:2017*; Concrete—Determination of the Resistance to the Degrade Due to Freeze-Thaw Cycles. European Committee for Standardization: Brussels, Belgium, 2017.
75. Nedeljković, M.; Visser, J.; Šavija, B.; Valcke, S.; Schlangen, E. Use of fine recycled concrete aggregates in concrete: A critical review. *J. Build. Eng.* **2021**, *38*, 102196. [[CrossRef](#)]
76. Corinaldesi, V.; Giuggiolini, M.; Moriconi, G. Use of rubble from building demolition in mortars. *Waste Manag.* **2002**, *22*, 893–899. [[CrossRef](#)]
77. Corinaldesi, V. Mechanical behavior of masonry assemblages manufactured with recycled-aggregate mortars. *Cem. Concr. Compos.* **2009**, *31*, 505–510. [[CrossRef](#)]
78. De Juan, M.S.; Gutiérrez, P.A. Study on the influence of attached mortar content on the properties of recycled concrete aggregate. *Constr. Build. Mater.* **2009**, *23*, 872–877. [[CrossRef](#)]
79. López-Gayarre, F.; Serna, P.; Domingo-Cabo, A.; Serrano-López, M.A.; López-Colina, C. Influence of recycled aggregate quality and proportioning criteria on recycled concrete properties. *Waste Manag.* **2009**, *29*, 3022–3028. [[CrossRef](#)]
80. Gómez-Soberón, J.M. Porosity of recycled concrete with substitution of recycled concrete aggregate: An experimental study. *Cem. Concr. Res.* **2002**, *32*, 1301–1311. [[CrossRef](#)]
81. Poon, C.S.; Shui, Z.H.; Lam, L. Effect of microstructure of ITZ on compressive strength of concrete prepared with recycled aggregates. *Constr. Build. Mater.* **2004**, *18*, 461–468. [[CrossRef](#)]
82. Etxeberria, M.; Vázquez, E.; Mari, A. Microstructure analysis of hardened recycled aggregate concrete. *Mag. Concr. Res.* **2006**, *58*, 683–690. [[CrossRef](#)]

83. Zhang, Y.; Wang, Y.; Li, T.; Xiong, Z.; Sun, Y. Effects of lithium carbonate on performances of sulphoaluminate cement-based dual liquid high water material and its mechanisms. *Constr. Build. Mater.* **2018**, *161*, 374–380. [[CrossRef](#)]
84. Telesca, A.; Marroccoli, M.; Coppola, L.; Coffetti, D.; Candamano, S. Tartaric acid effects on hydration development and physico-mechanical properties of blended calcium sulphoaluminate cements. *Cem. Concr. Compos.* **2021**, *124*, 104275. [[CrossRef](#)]
85. Torkittikul, P.; Chaipanich, A. Utilization of ceramic waste as fine aggregate within Portland cement and fly ash concretes. *Cem. Concr. Compos.* **2010**, *32*, 440–449. [[CrossRef](#)]
86. Thomson, M.; Lindqvist, J.E.; Elsen, J.; Groot, C.J.W.P. *2.5 Porosity of Mortars. Report 28: Characterisation of Old Mortars with Respect to their Repair-State-of-the-Art Report of RILEM Technical Committee 167-COM*; RILEM Publications: Bagneux, France, 2007; Volume 28, p. 75.
87. Mao, Y.; Liu, J.; Shi, C. Autogenous shrinkage and drying shrinkage of recycled aggregate concrete: A review. *J. Clean. Prod.* **2021**, *295*, 126435. [[CrossRef](#)]
88. Wu, J.; Jing, X.; Wang, Z. Uni-Axial compressive stress-strain relation of recycled coarse aggregate concrete after freezing and thawing cycles. *Constr. Build. Mater.* **2017**, *134*, 210–219. [[CrossRef](#)]
89. Li, Y.; Wang, R.; Li, S.; Zhao, Y. Assessment of the freeze–thaw resistance of concrete incorporating carbonated coarse recycled concrete aggregates. *J. Ceram. Soc. Jpn.* **2017**, *125*, 837–845. [[CrossRef](#)]
90. Cheng, Y.; Shang, X.; Zhang, Y. Experimental research on durability of recycled aggregate concrete under freeze-thaw cycles. *J. Phys. Conf. Ser.* **2017**, *870*, 012018. [[CrossRef](#)]
91. Li, Y.; Wang, R.; Zhao, Y. Effect of coupled deterioration by freeze-thaw cycle and carbonation on concrete produced with coarse recycled concrete aggregates. *J. Ceram. Soc. Jpn.* **2017**, *125*, 36–45. [[CrossRef](#)]
92. Júnior, N.A.; Silva, G.A.O.; Ribeiro, D.V. Effects of the incorporation of recycled aggregate in the durability of the concrete submitted to freeze-thaw cycles. *Constr. Build. Mater.* **2018**, *161*, 723–730. [[CrossRef](#)]
93. Richardson, A.; Coventry, K.; Bacon, J. Freeze/thaw durability of concrete with recycled demolition aggregate compared to virgin aggregate concrete. *J. Clean Prod.* **2011**, *19*, 272–277. [[CrossRef](#)]
94. Cao, W.L.; Liang, M.B.; Dong, H.Y.; Zhang, J.W. Experimental study on basic mechanical properties of recycled concrete after freeze–thaw cycles. *J. Nat. Disasters* **2012**, *21*, 184–190.
95. Zou, C.Y.; Fan, Y.H.; Hu, Q. Experimental study on the basic mechanical property of recycled concrete after freeze–thaw. *Build. Struct.* **2010**, *40*, 434–438.
96. Algourdin, N.; Nguyen, Q.N.A.; Mesticou, Z.; Larbi, A.S. Durability of recycled fine mortars under freeze–thaw cycles. *Constr. Build. Mater.* **2021**, *291*, 123330. [[CrossRef](#)]
97. Rangel, C.S.; Amario, M.; Pepe, M.; Martinelli, E.; Filho, R.D.T. Durability of structural recycled aggregate concrete subjected to freeze-thaw cycles. *Sustainability* **2020**, *12*, 6475. [[CrossRef](#)]
98. Müllauer, W.; Beddoe, R.E.; Heinz, D. Sulfate attack expansion mechanisms. *Cem. Concr. Res.* **2013**, *52*, 208–215. [[CrossRef](#)]
99. Bizzozero, J.; Gosselin, C.; Scrivener, K.L. Expansion mechanisms in calcium aluminate and sulfoaluminate systems with calcium sulfate. *Cem. Concr. Res.* **2014**, *56*, 190–202. [[CrossRef](#)]
100. Dhir, R.K.; Limbachiya, M.C.; Leelawat, T. BS 5328, BS 882. Suitability of recycled concrete aggregate for use in BS 5328 designated mixes. *Proc. Inst. Civ. Eng.-Struct. Build.* **1999**, *134*, 257–274. [[CrossRef](#)]
101. Bulatović, V.; Melešev, M.; Radeka, M.; Radonjanin, V.; Lukić, I. Evaluation of sulfate resistance of concrete with recycled and natural aggregates. *Constr. Build. Mater.* **2017**, *152*, 614–631. [[CrossRef](#)]
102. Bai, J. Durability of sustainable construction materials. In *Sustainability of Construction Materials*; Woodhead Publishing: Cambridge, MA, USA, 2016; pp. 397–414.
103. Tang, S.W.; Yao, Y.; Andrade, C.; Li, Z.J. Recent durability studies on concrete structure. *Cem. Concr. Res.* **2015**, *78*, 143–154. [[CrossRef](#)]
104. Santillán, L.R.; Locati, F.; Villagrán-Zaccardi, Y.A.; Zega, C.J. Long-Term sulfate attack on recycled aggregate concrete immersed in sodium sulfate solution for 10 years. *Mater. Constr.* **2020**, *70*, e212. [[CrossRef](#)]
105. Boudali, S.; Kerdal, D.E.; Ayed, K.; Abdulsalam, B.; Soliman, A.M. Performance of self-compacting concrete incorporating recycled concrete fines and aggregate exposed to sulphate attack. *Constr. Build. Mater.* **2016**, *124*, 705–713. [[CrossRef](#)]
106. Poole, A.B.; Thomas, A. A staining technique for the identification of sulphates in aggregates and concretes. *Mineral. Mag.* **1975**, *40*, 315–316. [[CrossRef](#)]
107. Xuan, D.X.; Shui, Z.H. Temperature dependence of thermal induced mesocracks around limestone aggregate in normal concrete. *Fire Mater. Int. J.* **2010**, *34*, 137–146. [[CrossRef](#)]
108. Li, B.; Zhang, Y.; Selyutina, N.; Smirnov, I.; Deng, K.; Liu, Y.; Miao, Y. Thermally-Induced mechanical degradation analysis of recycled aggregate concrete mixed with glazed hollow beads. *Constr. Build. Mater.* **2021**, *301*, 124350. [[CrossRef](#)]
109. Dündar, B.; Çınar, E.; Çalışkan, A.N. An investigation of high temperature effect on pumice aggregate light mortars with brick flour. *Res. Eng. Struct. Mat.* **2020**, *6*, 241–255. [[CrossRef](#)]
110. Hernández, M.G.; Anaya, J.J.; Izquierdo, M.A.G.; Ullate, L.G. Application of micromechanics to the characterization of mortar by ultrasound. *Ultrasonics* **2002**, *40*, 217–221. [[CrossRef](#)]
111. Flores-Ales, V.; Alducin-Ochoa, J.M.; Martín-del-Río, J.J.; Torres-Gonzalez, M.; Jimenez-Bayarri, V. Physical-Mechanical behaviour and transformations at high temperature in a cement mortar with waste glass as aggregate. *J. Build. Eng.* **2020**, *29*, 101158. [[CrossRef](#)]

112. Guo, M.Z.; Chen, Z.; Ling, T.C.; Poon, C.S. Effects of recycled glass on properties of architectural mortar before and after exposure to elevated temperatures. *J. Clean. Prod.* **2015**, *101*, 158–164. [[CrossRef](#)]
113. Heap, M.J.; Lavallée, Y.; Laumann, A.; Hess, K.U.; Meredith, P.G.; Dingwell, D.B.; Huismann, S.; Weise, F. The influence of thermal-stressing (up to 1000 C) on the physical, mechanical, and chemical properties of siliceous-aggregate, high-strength concrete. *Constr. Build. Mater.* **2013**, *42*, 248–265. [[CrossRef](#)]
114. Sarhat, S.R.; Sherwood, E.G. Residual mechanical response of recycled aggregate concrete after exposure to elevated temperatures. *J. Mater. Civ. Eng.* **2013**, *25*, 1721–1730. [[CrossRef](#)]
115. Khaliq, W. Mechanical and physical response of recycled aggregates high-strength concrete at elevated temperatures. *Fire Saf. J.* **2018**, *96*, 203–214. [[CrossRef](#)]